# Adjoint-based Aerodynamic and Aerostructural Optimization of Transport Aircraft

Gaetan K.W. Kenway
Joaquim R. R. A. Martins
University of Michigan
Department of Aerospace Engineering, Ann Arbor, MI

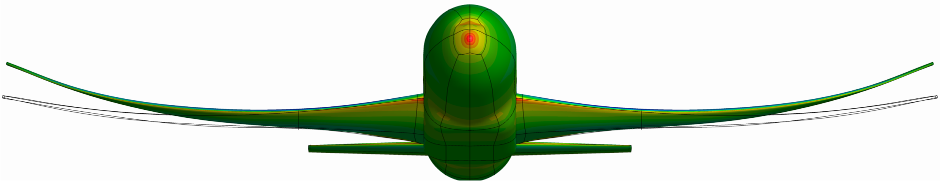

Advanced Modeling and Simulation Seminar Series
NASA Ames Research Center, February 7, 2017

# With over 90 000 flights daily, small improvements in commercial aircraft performance can have a huge impact

# The Boeing 707 and the Boeing 787 do not appear to have vastly different designs...


# Over 80% reduction in fuel burn of current generation compared to first generation jets

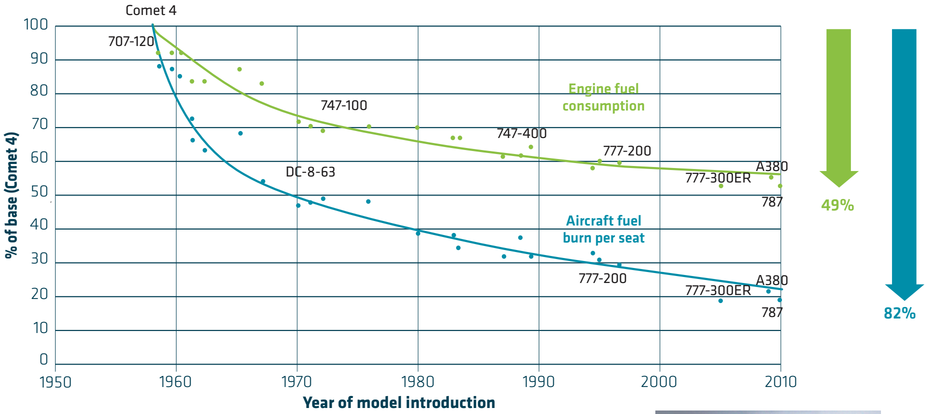


# Where will the next 80% fuel burn reduction come from?

# The next generation of transport aircraft will be more challenging to design

- High aspect ratio, flexible wings
- Coupled aero-propulsion effects from boundary layer ingestion
- Complex non-linear flutter behavior for truss-braced wings
- Unknown design space
- High risk


# Challenges for high-fidelity optimization in aircraft design

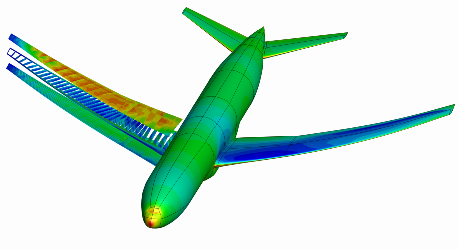

- Computational expensive objective and constraints
- Multiple high-coupled systems
- Large number of design variables, design points and constraints

# Outline

- Motivation
- Computing derivatives
- Aerodynamic shape optimization
- Aerostructural design optimization
- Summary

# Outline

- Motivation
- **Computing derivatives**
- Aerodynamic shape optimization
- Aerostructural design optimization
- Summary

# Gradient based optimization is our only hope for large numbers of design variables

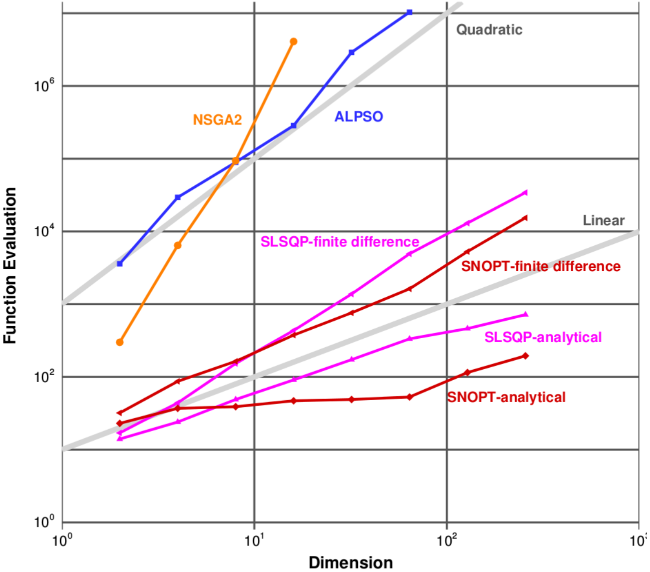

# Gradient-based optimization requires derivatives of the objective and constraints

$$\begin{aligned} \min \quad & f(x, y(x)) \\ \text{s.t} \quad & h(x, y(x)) = 0 \\ & g(x, y(x)) \leq 0 \end{aligned}$$

$x$: design variables

$y$: state variables. Determined by solving $\mathcal{R}(x, y(x)) = 0$

Need to find $\frac{\mathrm{d}f}{\mathrm{d}x}$ (and $\frac{\mathrm{d}h}{\mathrm{d}x}$, $\frac{\mathrm{d}g}{\mathrm{d}x}$)

# Method for computing derivatives

| | | |
|---|---|---|
| Monolithic<br>***Black boxes input and outputs*** | Finite-differences | $\frac{\mathrm{d}f}{\mathrm{d}x_j} = \frac{f(x_j + h) - f(x)}{h} + \mathcal{O}(h)$ |
| | Complex-step | $\frac{\mathrm{d}f}{\mathrm{d}x_j} = \frac{\mathrm{Im}\left[f(x_j + ih)\right]}{h} + \mathcal{O}(h^2)$ |
| Analytic<br>***Governing eqns state variables*** | Direct | $\frac{\mathrm{d}f}{\mathrm{d}x} = \frac{\partial f}{\partial x} - \underbrace{\frac{\partial f}{\partial y}\overbrace{\left[\frac{\partial R}{\partial y}\right]^{-1}}^{-\mathrm{d}y/\mathrm{d}x}}_{\psi}\frac{\partial R}{\partial x}$ |
| | Adjoint | |
| Algorithmic differentiation<br>***Lines of code code variables*** | Forward | $\begin{bmatrix} 1 & 0 & \dots & 0 \\ -\frac{\partial T_2}{\partial t_1} & 1 & \ddots & \vdots \\ \vdots & \ddots & \ddots & 0 \\ -\frac{\partial T_n}{\partial t_1} & \dots & -\frac{\partial T_n}{\partial t_{n-1}} & 1 \end{bmatrix} \begin{bmatrix} 1 & 0 & \dots & 0 \\ \frac{\mathrm{d}t_2}{\mathrm{d}t_1} & 1 & \ddots & \vdots \\ \vdots & \ddots & \ddots & 0 \\ \frac{\mathrm{d}t_n}{\mathrm{d}t_1} & \dots & \frac{\mathrm{d}t_n}{\mathrm{d}t_{n-1}} & 1 \end{bmatrix} = \boldsymbol{I} = \begin{bmatrix} 1 & -\frac{\partial T_2}{\partial t_1} & \dots & -\frac{\partial T_n}{\partial t_1} \\ 0 & 1 & \ddots & \vdots \\ \vdots & \ddots & \ddots & -\frac{\partial T_n}{\partial t_{n-1}} \\ 0 & \dots & 0 & 1 \end{bmatrix} \begin{bmatrix} 1 & \frac{\mathrm{d}t_2}{\mathrm{d}t_1} & \dots & \frac{\mathrm{d}t_n}{\mathrm{d}t_1} \\ 0 & 1 & \ddots & \vdots \\ \vdots & \ddots & 1 & \frac{\mathrm{d}t_n}{\mathrm{d}t_{n-1}} \\ 0 & \dots & 0 & 1 \end{bmatrix}$ |
| | Reverse | |

# Compute derivatives by linearizing the governing equations

Need $df/dx$ , $f(x, y(x))$

$$\frac{df}{dx} = \frac{\partial f}{\partial x} + \frac{\partial f}{\partial y}\frac{dy}{dx}$$

Derivative of the governing equations: $\mathcal{R}(x, y(x)) = 0$

$$\frac{\mathrm{d}\mathcal{R}}{\mathrm{d}x} = \frac{\partial \mathcal{R}}{\partial x} + \frac{\partial \mathcal{R}}{\partial y}\frac{\mathrm{d}y}{\mathrm{d}x} = 0 \rightarrow \frac{\partial \mathcal{R}}{\partial y}\frac{\mathrm{d}y}{\mathrm{d}x} = -\frac{\partial \mathcal{R}}{\partial x}$$

Substitute the result into the derivative equation

$$\frac{\mathrm{d}f}{\mathrm{d}x} = \frac{\partial f}{\partial x} \underbrace{- \frac{\partial f}{\partial y}\left[\frac{\partial \mathcal{R}}{\partial y}\right]^{-1}}_{\psi} \frac{\partial \mathcal{R}}{\partial x}$$

# Partial derivative terms evaluated using Automatic Differentiation (AD)

Solve the governing equations

$$\mathcal{R}\left(x, y(x)\right) = 0$$

Solve the adjoint equations for the particular function of interest, $f$

$$\left[\frac{\partial \mathcal{R}}{\partial y}\right]^T \psi = -\frac{\partial f}{\partial y}$$

and compute the derivatives

$$\frac{\mathrm{d}f}{\mathrm{d}x} = \frac{\partial f}{\partial x} + \psi^T \frac{\partial \mathcal{R}}{\partial x}$$

# Our requirements for using AD

- Yield derivatives **consistent** with the flow solution and be verifiable with the complex step
- Require **no modification** to the original code.
- Require **no duplication** of the original code.
- Result in an **efficient adjoint** derivative computation.
- Have an **automatic implementation**.
- Incur **no nonlinear run-time penalty**
- **Low memory** footprint.

# Adjoint approach with AD has evolved through four approaches

1. **Single Cell**: AD cell residual routine, loop over cells to assemble full Jacobian [2005]
2. **Forward mode coloring**: AD original residual routines using coloring for efficiency and store full Jacobian [2011]
3. **Full reverse mode**: AD master ghost routing that yields the desired transposed Jacobian-vector products in a matrix-free fashion [2014]
4. **Hybrid reverse mode**: AD individual non-linear routines and assemble the transposed Jacobian-vector productions manually [2015]

# Outline

- Motivation
- Computing derivatives
- **Aerodynamic shape optimization**
- Aerostructural design optimization
- Summary

# Small changes in shape can make a big difference in performance

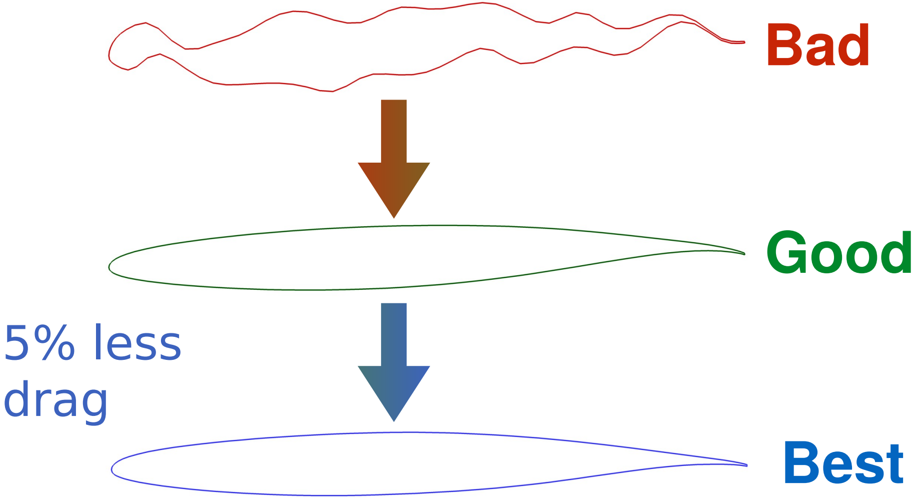

# Transonic aerodynamic shape optimization requires a high-fidelity model

# ADflow is well suited for optimization studies

- Parallel, $2^{nd}$ order, finite-volume multiblock/overset solver for the RANS equations
- SA and SST turbulence models
- Exact discrete adjoint implemented using AD
- Linearized turbulence model
- Newton–Krylov solution method for extremely rapid convergence

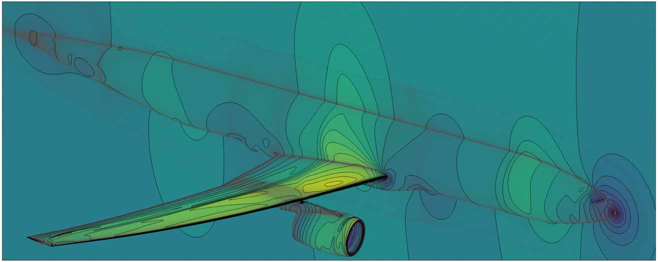

# Newton–Krylov method especially useful for optimization

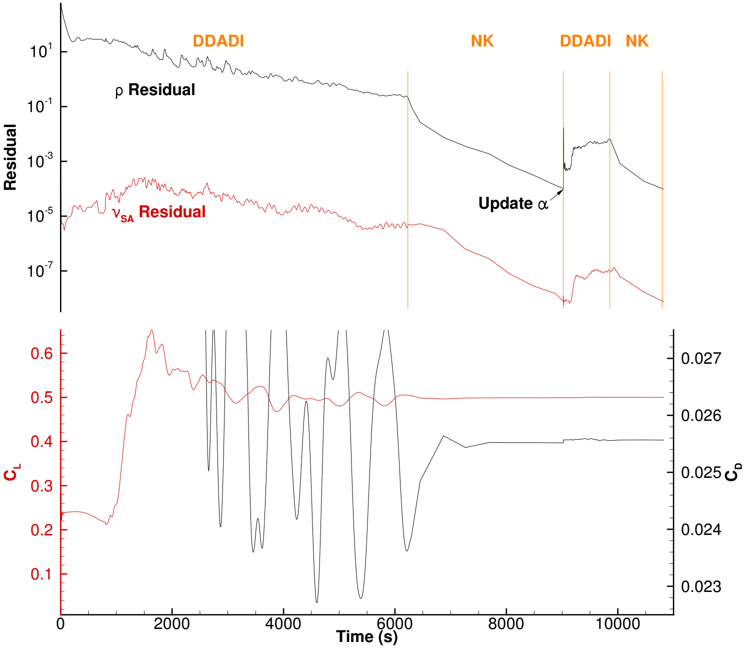

# Design optimization requires mores than just a flow solver

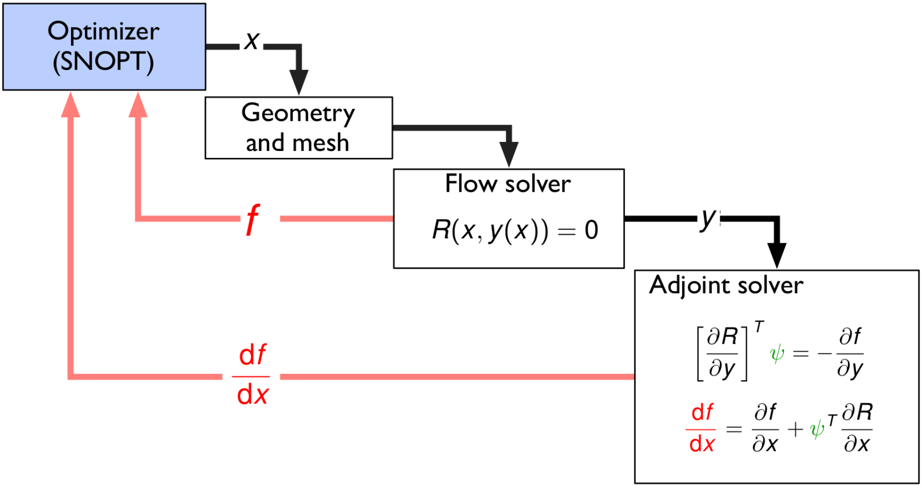

# Multiblock free-form deformation volume approach for complex configurations

- Visualized as embedding an object in a clear, flexible, rubber-like material
- $\mathbf{R}^3 \rightarrow \mathbf{R}^3$ B-spline basis mapping
- Smooth with global and local shape control
- Common parametrization for all disciplines

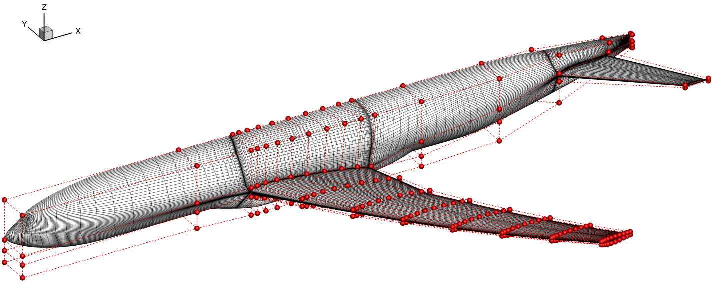

# Fast mesh deformation handles large design changes

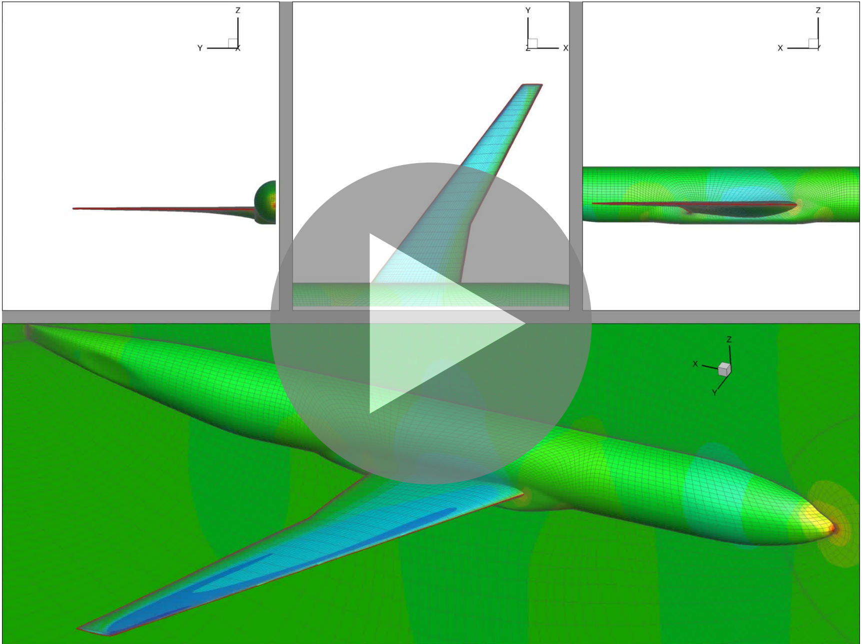

# ADODG Case 5: The CRM Wing-Body-Tail Configuration

- Nominal operating point: Mach=0.85, $C_L$=0.5
- Off design conditions: M=0.85, $C_L$=0.65; M=0.89, $C_L$=0.456
- Flight Reynolds number: $43 \times 10^6$
- Weighted drag minimization at fixed lift
- Trimmed flight conditions with tail control variable
- 100% minimum thickness constraints
- No decrease in wing initial volume

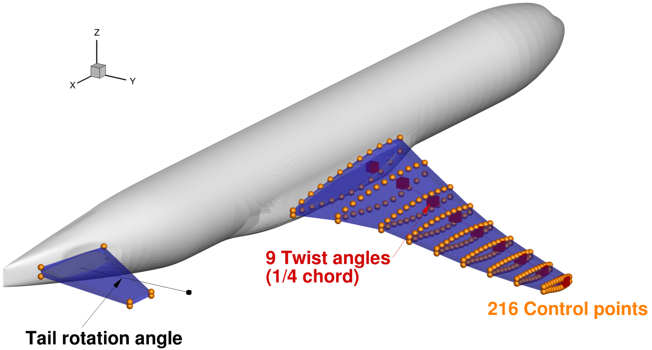

# "Separation sensor" method for buffet onset prediction

- Separated flow correlates with lowering of the lift curve slope
- Integral of area where $x$-axis component skin friction is negative

$$\text{Sep} = \frac{1}{A_{\text{ref}}} \iint_S \frac{1.0}{1.0 + e^{-2k(\chi-\lambda)}} dS$$

$$\chi = -\vec{V} \cdot \vec{V}_{\text{freestream}}$$

- Smooth Heaviside function ($k$=10)

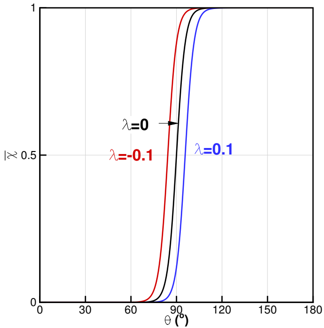

# Buffet onset for the CRM at M=0.85

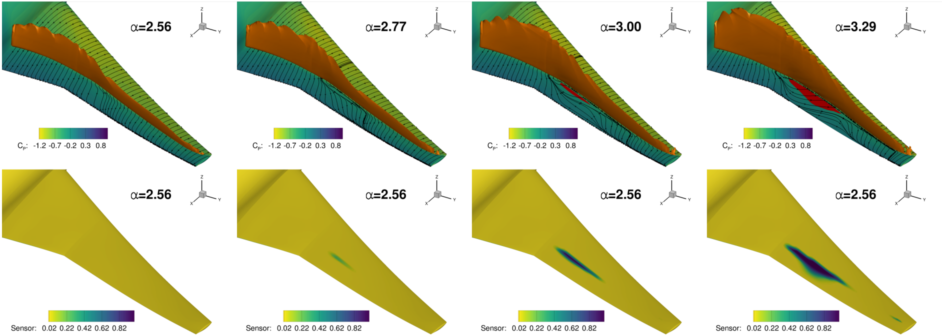


Red surface denotes flow in the negative stream-wise direction.
The brown isosurface is the Lovely–Haines shock sensor.

# ADODG Case 5 problem statement

| | | |
|---|---|---|
| minimize | $\sum_{i=1}^{N} \mathcal{W}_i C_{D_i}$ | Quantity |
| with respect to | Wing cross sectional shape | 240 |
| | Wing twist | 9 |
| | Angle of attack ($\alpha_i$) | N |
| | Tail rotation angle ($\eta_i$) | N |
| subject to | $C_{L_i} - C^*_{L_i} = 0.0$ | N |
| | $C_{M_{y_i}} = 0.0$ | N |
| | $t_j \geq t_{j_{\text{CRM}}}$ | 750 |

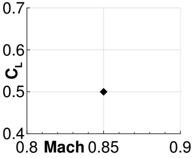


Case 5.1 (N=1)

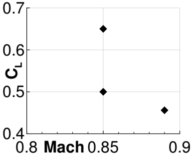


Case 5.2 (N=3)

# Case 5.1: Single point optimized design characteristics

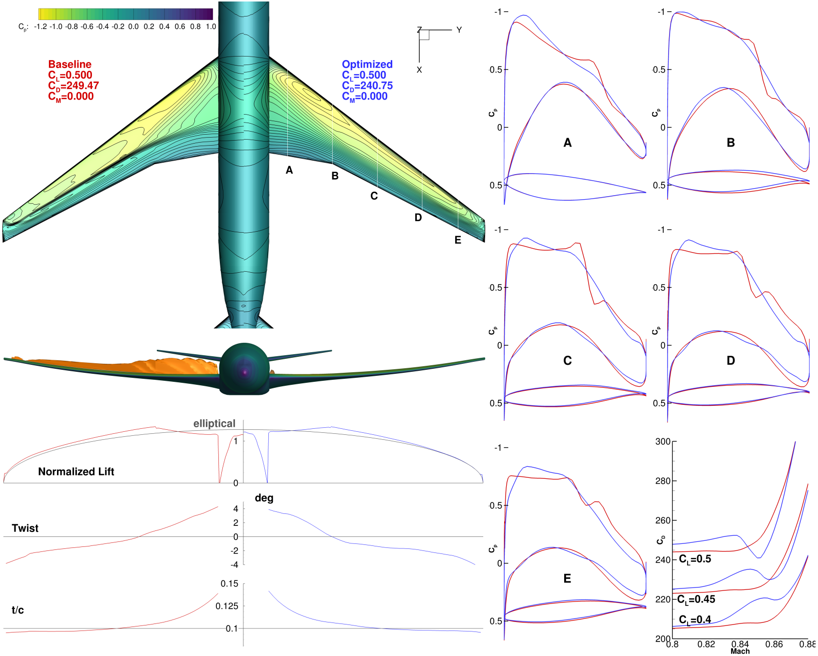

# Case 5.2: Off design conditions improve robustness

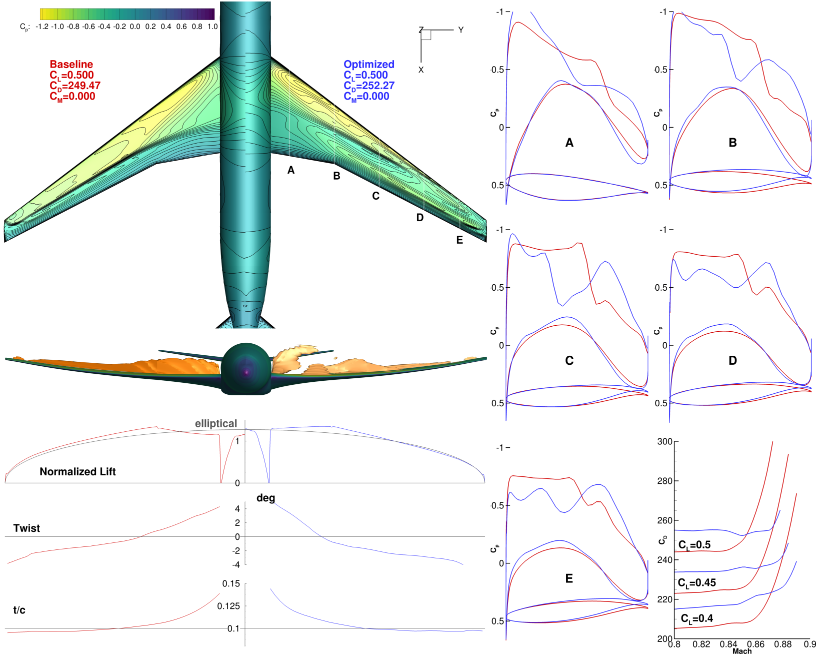

# ML/D contours give clear indication of off-design performance

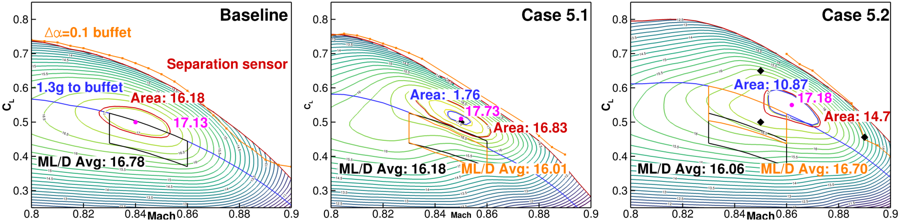


Buffet onset boundary

$\Delta\alpha = 0.1$ buffet onset boundary

1.3 g margin to buffet

99% $ML/D_{max}$ of baseline

99% $ML/D_{max}$

Absolute maximum ML/D

Integration region based on actual 1.3 g margin

Integration region based on baseline 1.3 g margin

# Off-design weighting or buffet-onset constraint?

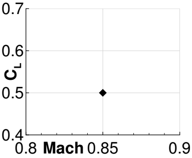


Case 5.1

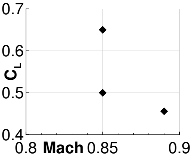


Case 5.2

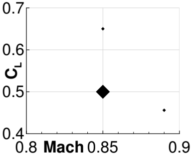


Case 5.3

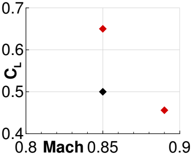


Case 5.4

# Case 5.3 and Case 5.4 still result in unsatisfactory designs

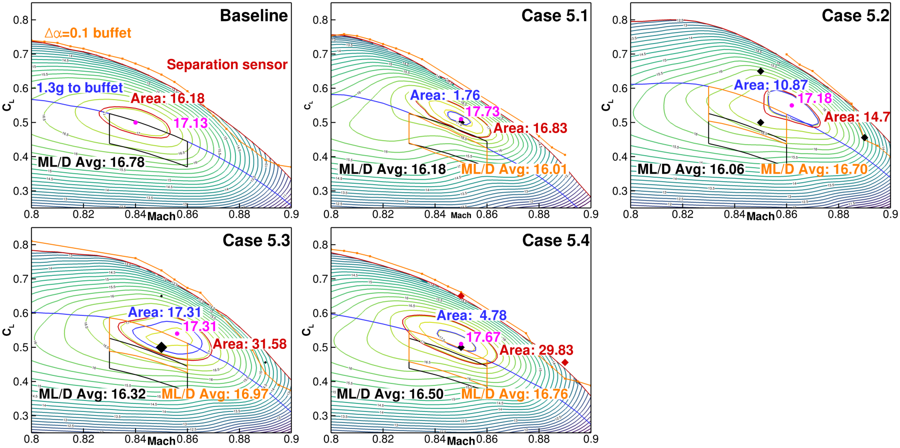

# Will multipoint formulations help?

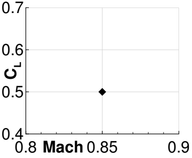


Case 5.1

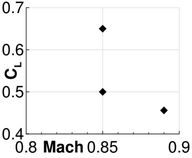


Case 5.2

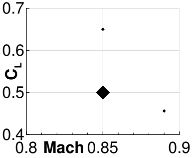


Case 5.3

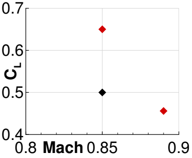


Case 5.4

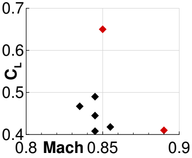


Case 5.5

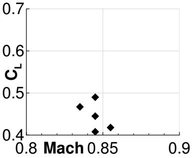


Case 5.6

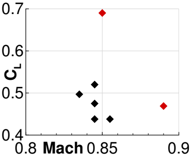


Case 5.7

$ML/D$ Maximization with variable $C_L$.

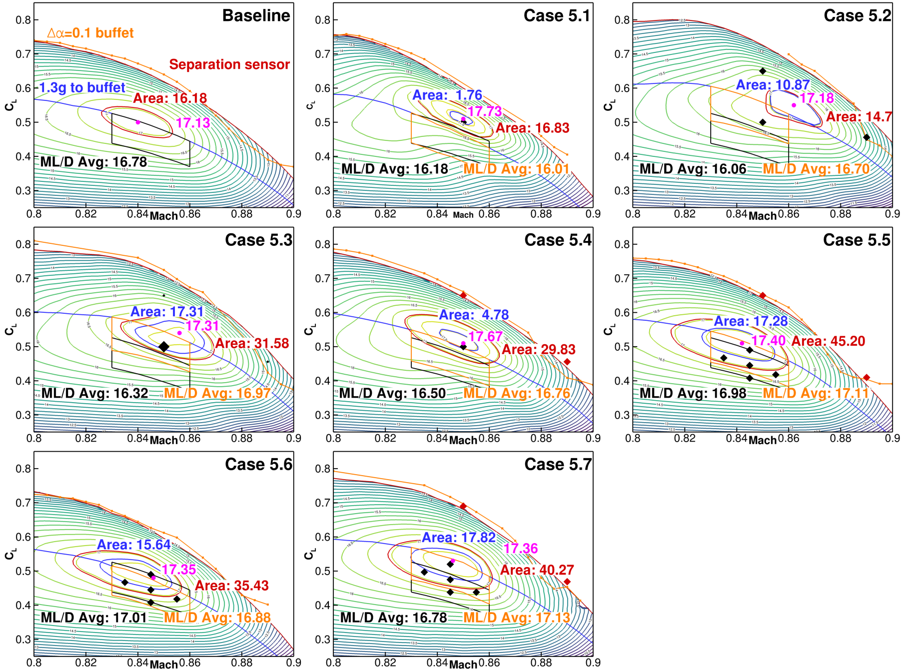
Baseline
Δα=0.1 buffet
Separation sensor
1.3g to buffet
Area: 16.18
17.13
ML/D Avg: 16.78
Case 5.1
Area: 1.76
17.73
Area: 16.83
ML/D Avg: 16.18
ML/D Avg: 16.01
Case 5.2
Area: 10.87
17.18
Area: 14.7
ML/D Avg: 16.06
ML/D Avg: 16.70
Case 5.3
Area: 17.31
17.31
Area: 31.58
ML/D Avg: 16.32
ML/D Avg: 16.97
Case 5.4
Area: 4.78
17.67
Area: 29.83
ML/D Avg: 16.50
ML/D Avg: 16.76
Case 5.5
Area: 17.28
17.40
Area: 45.20
ML/D Avg: 16.98
ML/D Avg: 17.11
Case 5.6
Area: 15.64
17.35
Area: 35.43
ML/D Avg: 17.01
ML/D Avg: 16.88
Case 5.7
Area: 17.82
17.36
Area: 40.27
ML/D Avg: 16.78
ML/D Avg: 17.13
Mach
C_L

# Computational cost breakdown in CPU-hours

- Intel E5540 CPUs running at 2.66 GHz

| Case | L2 optimization | L1.5 optimization | Contour | Grid convergence | Total |
|---|---|---|---|---|---|
| Baseline | – | – | 1 346 | 817 | 2 162 |
| 5.1 | 289 | 611 | 1 270 | 1 009 | 3 179 |
| 5.2 | 2 378 | 2 394 | 1 795 | 1 121 | 7 688 |
| 5.3 | 1 290 | 2 505 | 1 750 | 910 | 6 457 |
| 5.4 | 1 507 | 2 602 | 1 384 | 1 024 | 6 518 |
| 5.5 | 2,090 | 3 506 | 1 392 | 830 | 7 369 |
| 5.6 | 1,111 | 1 803 | 1 147 | 610 | 4 673 |
| 5.7 | 4,136 | 6 623 | 1 800 | 696 | 13 255 |
| Total | 12 802 | 19 567 | 11 886 | 7 019 | 51 303 |

# Outline

- Motivation
- Computing derivatives
- Aerodynamic shape optimization
- **Aerostructural design optimization**
- Summary

# Wing design is more than just aerodynamics

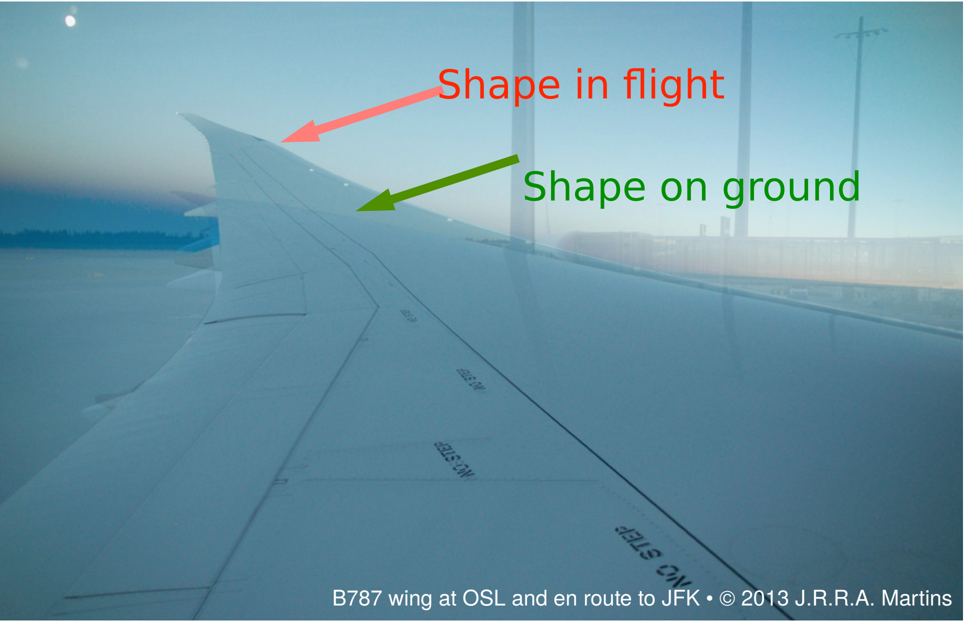


B787 wing at OSL and en route to JFK • © 2013 J.R.R.A. Martins

# Why you should not trust an aerodynamist (even a brilliant one) to make design decisions

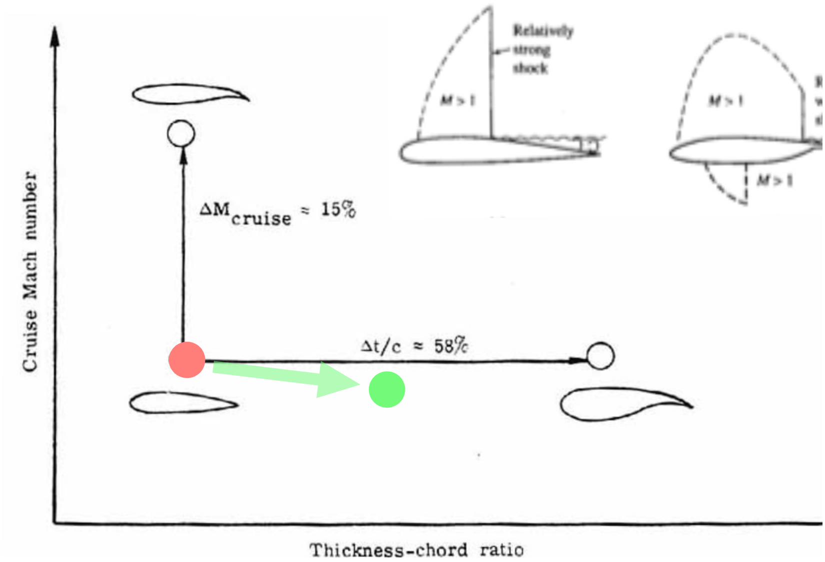


[NASA]

# Want to optimize both aerodynamic shape and structural sizing, with high fidelity

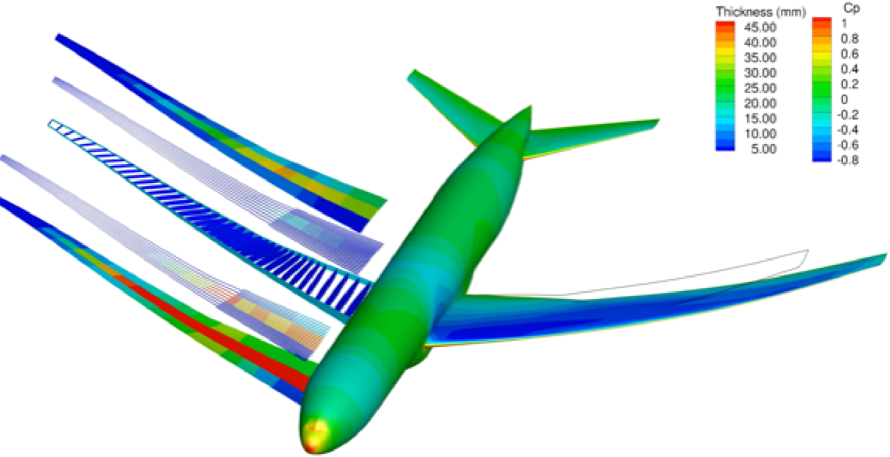

# MDO for Aircraft Configuration with High-fidelity (MACH)

<table>
<tr><td colspan="4">Python user script<br>Setup up the problem: objective function, constraints, design variables, optimizer and solver options</td></tr>
<tr><td colspan="2">Optimizer interface<br>*pyOptSparse*<br>Common interface to various optimization software</td><td colspan="2">Aerostructural solver<br>*AeroStruct*<br>Coupled solution methods and coupled derivative evaluation</td><td rowspan="2">Geometry modeler<br>*DVGeometry/GeoMACH*<br>Def nes and manipulates geometry, evaluates derivatives</td></tr>
<tr><td>SNOPT</td><td>Other optimizers</td><td>Structural solver<br>*TACS*<br>Governing and adjoint equations</td><td>Flow solver<br>*ADflow*<br>Governing and adjoint equations</td></tr>
</table>

- Underlying solvers are parallel and compiled
- Coupling through memory only
- Emphasis on clean Python user interface

# Structural Solver TACS:
# Toolkit for the Analysis of Composite Structures

- Linear finite element method with MITC shell elements
- Efficient parallel-direct solver for systems with millions of degrees of freedom
- Structural residuals: $\mathcal{S}(u) = 0$

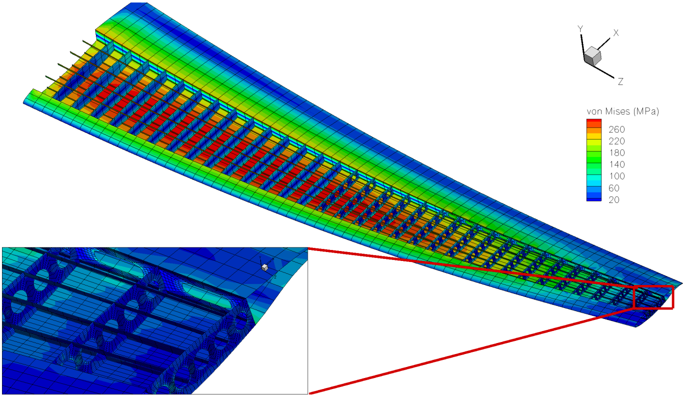

# Load and displacement transfer

- CFD loads must be transferred to the CSM model
- Rigid link approach for non-matching surfaces
- Design variable dependent, but robust

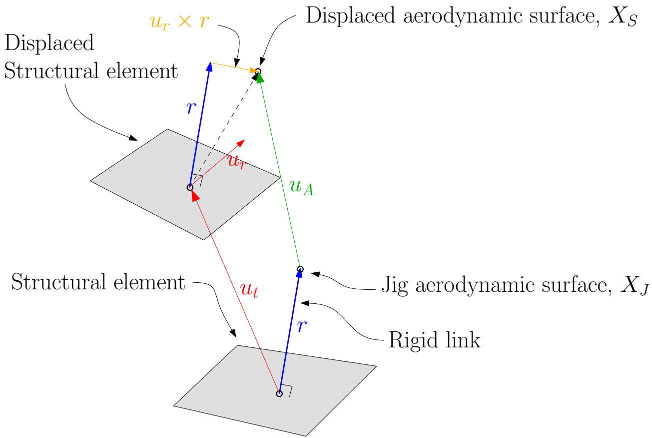

# Aerostructural solution techniques: Nonlinear Block Gauss–Seidel Method (NLBGS)

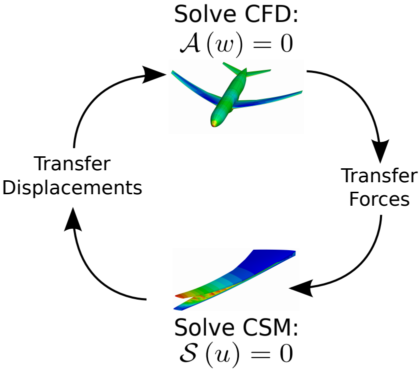


$\mathcal{A}$: Aerodynamic residuals
$w$: Aerodynamic states
$\mathcal{S}$: Structural residuals
$u$: Structural states

- Convergence can be accelerated with Aitken acceleration

$$\theta \leftarrow \theta \left( 1 - \frac{\left(\Delta u^{(k)} - \Delta u^{(k-1)}\right) \cdot \Delta u^{(k)}}{\| \left(\Delta u^{(k)} - \Delta u^{(k-1)}\right) \|^2} \right)$$

$$u^{(k+1)} \leftarrow u^{(k)} + \theta \Delta u^{(k)}$$

# Aerostructural solution techniques: Coupled Newton–Krylov Method (CNK)

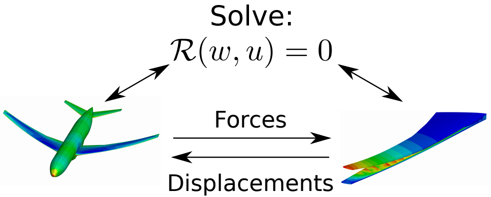


$\mathcal{R} = \begin{pmatrix} \mathcal{A}^T & \mathcal{S}^T \end{pmatrix}^T$: Aerostructural residuals

$w$: Aerodynamic states

$u$: Structural states

- Monolithic solution strategy – full aerostructural problem treated simultaneously
- Newton update:

$$\begin{bmatrix} \frac{\partial \mathcal{A}}{\partial w} & \frac{\partial \mathcal{A}}{\partial u} \\ \frac{\partial \mathcal{S}}{\partial w} & \frac{\partial \mathcal{S}}{\partial u} \end{bmatrix} \begin{bmatrix} \Delta w \\ \Delta u \end{bmatrix} = - \begin{bmatrix} \mathcal{A}(w) \\ \mathcal{S}(u) \end{bmatrix}$$

- Matrix-free FGMRES with Block–Jacobi preconditioner
- With wrapped codes and direct state/residual variable access, very little code modification!

# Adjoint method can be extended to aerostructural system

- Adjoint sensitivities are imperative for high-fidelity aerostructural optimization with large numbers of design variables
- For each function of interest, $I$, solve for the coupled adjoint vector, $\Psi = \begin{pmatrix}\psi^T & \phi^T\end{pmatrix}^T$:

$$\begin{bmatrix} \frac{\partial \mathcal{A}}{\partial w} & \frac{\partial \mathcal{A}}{\partial u} \\ \frac{\partial \mathcal{S}}{\partial w} & \frac{\partial \mathcal{S}}{\partial u} \end{bmatrix}^T \begin{bmatrix} \psi \\ \phi \end{bmatrix} = \begin{bmatrix} \frac{\partial I}{\partial w} & \frac{\partial I}{\partial u} \end{bmatrix}^T$$

- Adjoint vector is independent of the number design variables
- Solve one adjoint for each function
- Total sensitivity with respect to design variables, $x$, can then be obtained with

$$\frac{\mathrm{d}I}{\mathrm{d}x} = \frac{\partial I}{\partial x} - \psi^T \left(\frac{\partial \mathcal{A}}{\partial x}\right) - \phi^T \left(\frac{\partial \mathcal{S}}{\partial x}\right)$$

# Adjoint method efficiently computes gradients with respect to thousands of variables

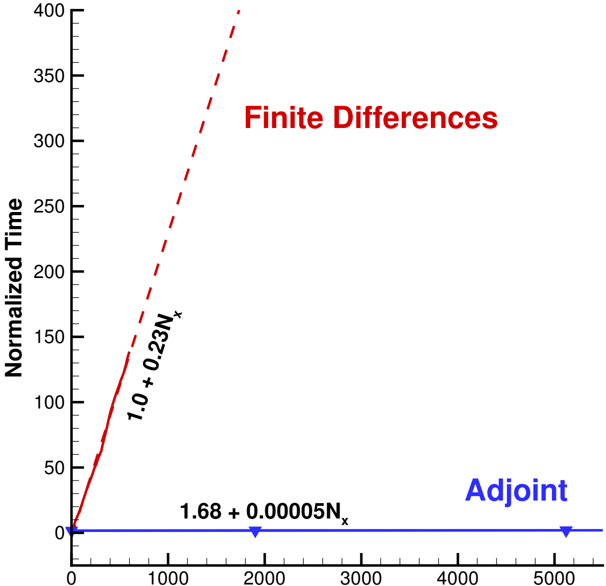

# Let's do aerostructural optimization!

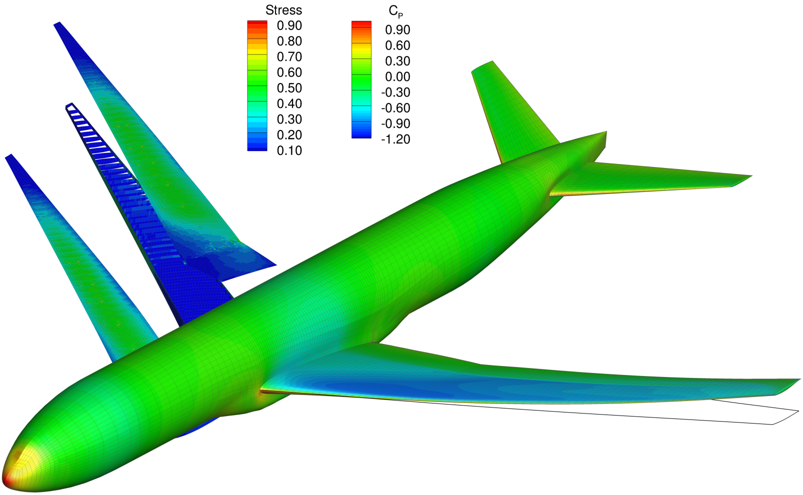


NASA-Michigan undeformed Common Research Model (uCRM)

# Optimize with respect to 972 “aerodynamic” and structural sizing variables

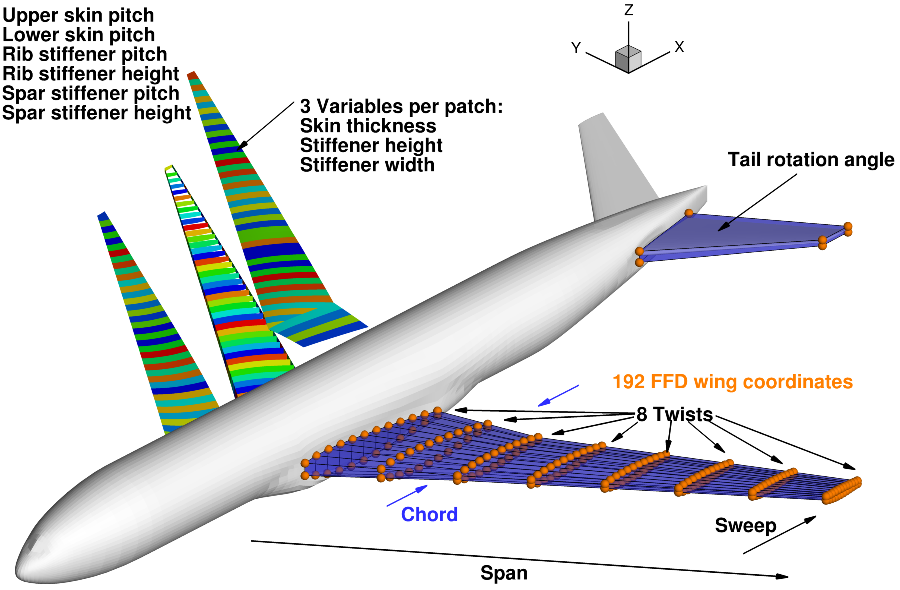

# Optimization objective and design variables

| | Function/variable | Description | Quantity |
|---|---|---|---|
| minimize | $\sum_i^N \mathcal{W}_i FB$ | | |
| with respect to | $x_{\text{span}}$ | Wing span | 1 |
| | $x_{\text{sweep}}$ | Wing sweep | 1 |
| | $x_{\text{chord}}$ | Wing chord | 1 |
| | $x_{\text{twist}}$ | Wing twist | 7 |
| | $x_{\text{airfoil}}$ | FFD control points | 192 |
| | $x_{\text{alpha}_i}$ | Angle of attack at each flight condition | 12 |
| | $x_{\eta_i}$ | Tail rotation angle at each flight condition | 12 |
| | $x_{\text{throttle}_i}$ | Throttle setting for each cruise flight condition | 7 |
| | $x_{\text{altitude}}$ | Cruise altitude | 1 |
| | $X_{\text{CG}}$ | CG position | 1 |
| | $x_{\text{skin pitch}}$ | Upper/lower stiffener pitch | 2 |
| | $x_{\text{spar pitch}}$ | LE/TE Spar stiffener pitch | 2 |
| | $x_{\text{ribs}}$ | Rib thickness | 45 |
| | $x_{\text{panel thick}}$ | Panel thickness skins/spars | 172 |
| | $x_{\text{stiff thick}}$ | Panel stiffener thickness skins/spars | 172 |
| | $x_{\text{stiff height}}$ | Panel stiffener height skins/spars | 172 |
| | $x_{\text{panel length}}$ | Panel length skin/spars | 172 |
| | | **Total design variables** | **972** |

# Constraints

| | Function/variable | Description | Quantity |
|---|---|---|---|
| subject to | $L = n_i W$ | Lift constraint | 12 |
| | $C_{M_{y_i}} = 0.0$ | Trim constraint | 12 |
| | $T = D$ | Thrust constraint | 7 |
| | $1.08D - T_{\max} < 0$ | Excess thrust constraint | 7 |
| | $t_{\mathrm{LE}}/t_{\mathrm{LE}_{\mathrm{Init}}} \geq 1.0$ | Leading edge radius | 20 |
| | $t_{\mathrm{TE}}/t_{\mathrm{TE}_{\mathrm{Init}}} \geq 1.0$ | Trailing edge thickness | 20 |
| | $\mathcal{V}_{\mathrm{wing}} > \mathcal{V}_{\mathrm{fuel}}$ | Minimum fuel volume | 1 |
| | $x_{\mathrm{CG}} - 1/4MAC = 0$ | CG location at 1/4 chord MAC | 1 |
| | $L_{\mathrm{panel}} - x_{\mathrm{panel\ length}} = 0$ | Target panel length | 172 |
| | $\mathrm{KS}_{\mathrm{stress}} \leq 1$ | 2.5 g Yield stress | 4 |
| | $\mathrm{KS}_{\mathrm{buckling}} \leq 1$ | 2.5 g Buckling | 3 |
| | $\mathrm{KS}_{\mathrm{buckling}} \leq 1$ | -1.0 g Buckling | 3 |
| | $\mathrm{KS}_{\mathrm{buckling}} \leq 1$ | 1.78 g Yield stress | 3 |
| | $\mathrm{KS}_{\mathrm{buckling}} \leq 1$ | 1.78 g Buckling | 4 |
| | $\left\lvert x_{\mathrm{panel\ thick}_i} - x_{\mathrm{panel\ thick}_{i+1}} \right\rvert \leq 0.005$ | Skin thickness adjacency | 168 |
| | $\left\lvert x_{\mathrm{stiff\ thick}_i} - x_{\mathrm{stiff\ thick}_{i+1}} \right\rvert \leq 0.005$ | Stiffener thickness adjacency | 168 |
| | $\left\lvert x_{\mathrm{stiff\ height}_i} - x_{\mathrm{stiff\ height}_{i+1}} \right\rvert \leq 0.005$ | Stiffener height adjacency | 168 |
| | $x_{\mathrm{stiff\ thick}} - x_{\mathrm{panel\ thick}} < 0.005$ | Maximum stiffener-skin difference | 172 |
| | $\Delta z_{\mathrm{TE,upper}} = -\Delta z_{\mathrm{TE,lower}}$ | Fixed trailing edge | 8 |
| | $\Delta z_{\mathrm{LE,upper}} = -\Delta z_{\mathrm{LE,lower}}$ | Fixed leading edge | 8 |
| | | **Total constraints** | **961** |

# Fewer geometric constraints are required for aerostructural optimization

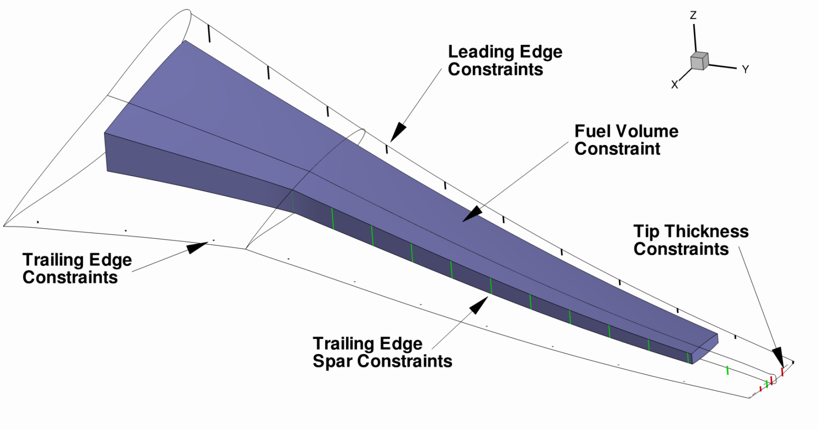

# Considering multiple flight conditions is required for a practical design

- 7 cruise conditions for performance
- 2 off-design buffet onset conditions
- 3 maneuver conditions for structural constraints
- All flight conditions trimmed

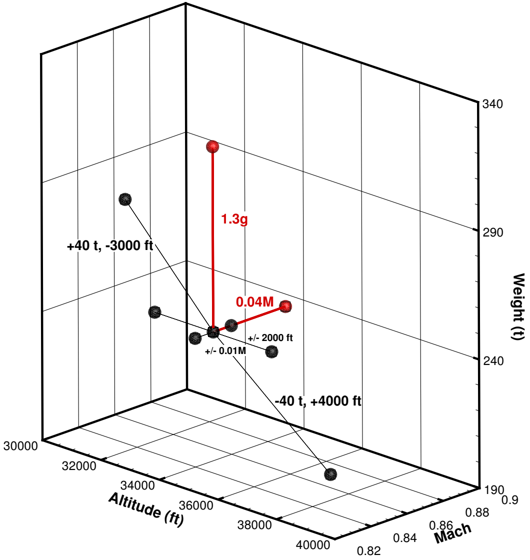

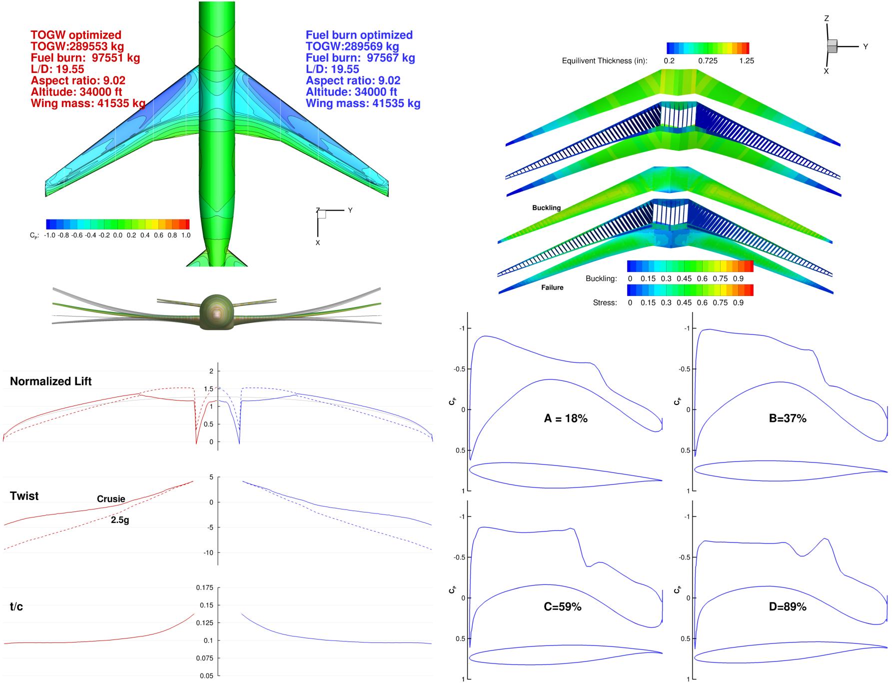

TOGW optimized
TOGW:289553 kg
Fuel burn: 97551 kg
L/D: 19.55
Aspect ratio: 9.02
Altitude: 34000 ft
Wing mass: 41535 kg
Fuel burn optimized
TOGW:289569 kg
Fuel burn: 97567 kg
L/D: 19.55
Aspect ratio: 9.02
Altitude: 34000 ft
Wing mass: 41535 kg
Cp: -1.0 -0.8 -0.6 -0.4 -0.2 0.0 0.2 0.4 0.6 0.8 1.0
Equilivent Thickness (in): 0.2 0.725 1.25
Buckling
Failure
Buckling: 0 0.15 0.3 0.45 0.6 0.75 0.9
Stress: 0 0.15 0.3 0.45 0.6 0.75 0.9
Normalized Lift
Twist
Crusie
2.5g
t/c
A = 18%
B=37%
C=59%
D=89%

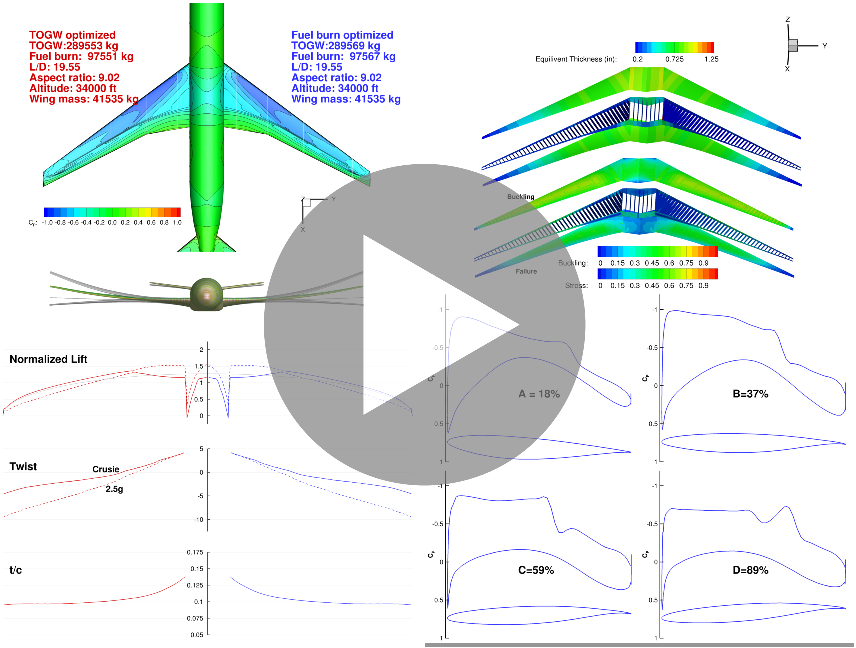

TOGW optimized
TOGW:289553 kg
Fuel burn: 97551 kg
L/D: 19.55
Aspect ratio: 9.02
Altitude: 34000 ft
Wing mass: 41535 kg
Fuel burn optimized
TOGW:289569 kg
Fuel burn: 97567 kg
L/D: 19.55
Aspect ratio: 9.02
Altitude: 34000 ft
Wing mass: 41535 kg
Equilivent Thickness (in): 0.2 0.725 1.25
Buckling
Failure
Buckling: 0 0.15 0.3 0.45 0.6 0.75 0.9
Stress: 0 0.15 0.3 0.45 0.6 0.75 0.9
Normalized Lift
Twist
Crusie
2.5g
t/c
A = 18%
B=37%
C=59%
D=89%

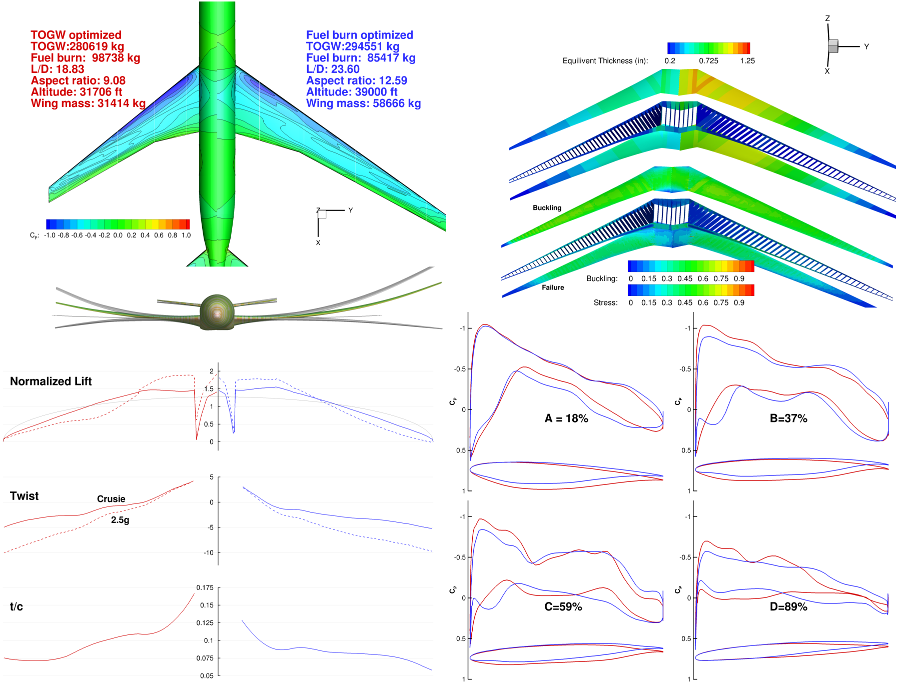

TOGW optimized
TOGW:280619 kg
Fuel burn: 98738 kg
L/D: 18.83
Aspect ratio: 9.08
Altitude: 31706 ft
Wing mass: 31414 kg
Fuel burn optimized
TOGW:294551 kg
Fuel burn: 85417 kg
L/D: 23.60
Aspect ratio: 12.59
Altitude: 39000 ft
Wing mass: 58666 kg
$C_p$: -1.0 -0.8 -0.6 -0.4 -0.2 0.0 0.2 0.4 0.6 0.8 1.0
Equilivent Thickness (in): 0.2 0.725 1.25
Buckling
Failure
Buckling: 0 0.15 0.3 0.45 0.6 0.75 0.9
Stress: 0 0.15 0.3 0.45 0.6 0.75 0.9
Normalized Lift
Twist
Crusie
2.5g
t/c
A = 18%
B=37%
C=59%
D=89%

# Outline

- Motivation
- Computing derivatives
- Aerodynamic shape optimization
- Aerostructural design optimization
- **Summary**

# Summary

- Efficient and accurate gradient computations via the adjoint method and automatic differentiation
- Dual challenge of expensive function evaluations with large number of design variables
- Aerodynamic shape optimization limits design space
- Extend the adjoint method to multiple disciplines
- Aerostructural design optimization with respect to 1000 design variables
- Still much more work to do!

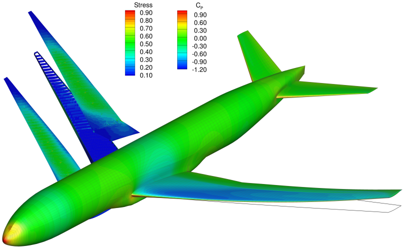

# Relevant publications


Graeme J. Kennedy and Joaquim R. R. A. Martins.
A parallel finite-element framework for large-scale gradient-based design optimization of high-performance structures.
*Finite Elements in Analysis and Design*, 87:56–73, September 2014.

Gaetan K. W. Kenway, Graeme J. Kennedy, and Joaquim R. R. A. Martins.
Scalable parallel approach for high-fidelity steady-state aeroelastic analysis and derivative computations.
*AIAA Journal*, 52(5):935–951, May 2014.

Gaetan K. W. Kenway and Joaquim R. R. A. Martins.
Multipoint high-fidelity aerostructural optimization of a transport aircraft configuration.
*Journal of Aircraft*, 51(1):144–160, January 2014.

Gaetan K. W. Kenway and Joaquim R. R. A. Martins.
Buffet onset constraint formulation for aerodynamic shape optimization.
*AIAA Journal*, 2017.
(In press).

Gaetan W. K. Kenway and Joaquim R. R. A. Martins.
High-fidelity aerostructural optimization considering buffet onset.
In *Proceedings of the 16th AIAA/ISSMO Multidisciplinary Analysis and Optimization Conference*, Dallas, TX, June 2015.
AIAA 2015-2790.

Joaquim R. R. A. Martins and John T. Hwang.
Review and unification of methods for computing derivatives of multidisciplinary computational models.
*AIAA Journal*, 51(11):2582–2599, November 2013.

# Questions

`mdolab.engin.mich.edu`

AEROSPACE ENGINEERING

UNIVERSITY of MICHIGAN